Characterization of Y Distributions and Nano-feature Formation In As Atomized, Milled, Milled and Annealed and Milled and Consolidated 14YWT Powders

N. J. Cunningham, Y. Wu, G. R. Odette and T. Yamamoto (University of California Santa Barbara)

SUMMARY

We report here on work supported by the DOE Office of Nuclear Energy that is complementary to our OFES work on nano-structured ferritic alloys (NFA) for fusion applications. Three variants of Fe14Cr3W0.4Ti0.2Y rapidly solidified powders were gas atomized by Crucible Research (CR) in Ar, Ar/O and He atmospheres. This work is part of an collaborative effort between CR, LANL, ORNL, UCSB, UC Berkeley and South Dakota School of Mines to develop larger heats of NFA using best practice processing routes. One objective was to determine if rapid solidification could introduce a uniform distribution of Y prior to mechanically alloying (MA), which is the standard method for mixing Y in NFA powders. The Y distribution in the powders was characterized by TEM, EPMA, APT and SANS in as atomized, ball milled and milled and annealed conditions. It was found that pre-alloying Y during gas atomization does not produce a uniform Y distribution. However, sufficient ball milling improves the homogeneity of the Y distribution. A bimodal grain size distribution was observed in the milled and annealed powders for all gas atomization atmospheres, and Y-Ti-O precipitates are present in both the large and small grains in sizes and quantities comparable to other NFA.

Introduction and Background

Nano-structured ferritic alloys (NFA) have high tensile and creep strength permitting operation up to 800°C, manifest remarkable resistance to radiation damage and can manage a high concentration of He [1]. These outstanding properties derive from an ultrahigh density of Ti-Y-O enriched nano-features (NF) that provide dispersion strengthening, help stabilize dislocation and fine grain structures, reduce excess concentrations of displacement defects and trap He in fine bubbles [1].

NFA are typically processed by MA rapidly solidified powders with Y_2O_3. The Y and O dissolve in the Fe matrix, subsequently precipitating with Ti during hot consolidation. However, the distribution of NF is often non-uniform, due to a corresponding non-uniform distribution of Y. Previous research suggested that the larger grains have a low density of NF [2].

Pre-alloying rapidly solidified powders with Y during gas atomization could, in principle, produce a more uniform dispersion of this element. If successful, this approach could significantly reduce, or even eliminate, ball milling times. Our specific objectives were to evaluate similarities and differences in three powder variants by characterizing the Y distribution in the as-atomized powders, following SPEX milling for 10 h and after annealing that mimics HIP consolidation temperature-time histories. The CR powders in the milled and annealed condition were also compared to conventional MA milled and annealed NFA powders and MA957.

Material and Methods

Three rapidly solidified powder variants with nominal composition (wt%) Fe-14Cr-3W-0.4Ti-0.2Y were acquired from CR. The variants involved gas atomization in different atmospheres - Ar, Ar/O, and He. The Ar atmosphere is standard. The Ar/O mixture was used to introduce a specified concentration of ≈ 0.15 wt% O. The higher thermal conductivity He atmosphere was intended to explore the effect of higher powder cooling rates on the Y distribution. Small charges of each powder variant were severely deformed in a SPEX shaker mill under the following conditions: 5:1 ball mass to charge ratio, 10h mill time, 100g ball mass and 8 mm ball diameters. A portion of the milled powder was then encapsulated, along with a Nb O getter foil, in a quartz tube and annealed at 1100°C for 3h in an inert He atmosphere with ramp rates of 15°C/min. Annealing is much more convenient and efficient than actual consolidation and previous research showed the NF formation is primarily dependent on temperature and time and not on consolidation [3].

A Cameca SX-50 electron probe micro-analyzer (EPMA) fitted with 5 wavelength spectrometers and a PGT X-ray energy dispersive detector was used to determine the Y content and distribution in the as-atomized powders, MA and MA and annealed powders. Fe, Cr, Ti, W, and O were also measured. The powder samples were mounted in a conductive polymer and polished on an Allied MultiPrep™ with a final polishing step using 0.05 µm colloidal silica. Three to five measurements, spaced ≈ 5 µm apart, were made on each particle with a total of 15 to 45 data points taken on 5 to 9 particles.

SANS measurements were performed at the NIST Center for Neutron Research (NCNR) facility in Gaithersburg, MD [4]. All measurements used a neutron wavelength of 5Å and a sample to detector distance of 1.547 m. Each powder sample was contained in a sealed, 1100 series aluminum holder with 7.4 mm diameter by 2 mm deep pocket with aluminum window thicknesses of 0.25 mm. The detector was offset in the horizontal direction to increase the q-range. The samples were placed inside a strong magnetic field of around 1.7 T to separate the magnetic scattering from the nuclear scattering. A minimum of 5 million detector counts was acquired for each sample run. The scattering cross sections for each sample were then found after subtracting background and empty container scattering and normalizing for each sample mass and measured transmission relative to a water standard. To allow quantitative analysis, scattering from a control specimen without Y-Ti-O NF was also measured and subtracted from the sample scattering. The control was a Fe14Cr3W0.3Ti rapidly solidified powder that was also SPEX milled for 10 h and annealed at 1100ºC for 3 h. Further details on the SANS analysis are given in Ref. [5].

TEM measurements were performed on an FEI Tecnai G2 Sphera Microscope. Following a procedure by Harris [6], M-Bond 610 epoxy was mixed with each powder sample, and after partially curing, the powders were punched into 3mm disks, dimple ground, and then dual ion beam polished using a Gatan 691 ion polishing system, first at 5 kV and incrementally stepped down to 2 kV. Using bright field imaging and energy dispersive x-ray spectroscopy (EDS), the grain size was observed and the composition of the large precipitates was measured.

Atom probe tomography (ATP) measurements were performed using an Imago 3000X HR Laser LEAP. The atom probe samples were micro-machined by an annular milling technique, described by Miller [7], from the Ar atomized milled and annealed sample, using an FEI Helios 600 dual beam FIB in conjunction with an Omniprobe Autoprobe 200 manipulator. The FIB SEM was also used to image the grain structures of the powders. The SEM also allowed selecting atom probe lift out samples from both the large and small grain regions. The atom probe was run in the laser mode with run parameters of 0.15 nJ laser pulse energy, 0.5-2% evaporation rate, 33.5 K temperature and a pulse frequency of 200kHz.

Results

EPMA analysis showed that pre-alloying Y during gas atomization does not produce a uniform Y distribution and that MA is necessary to improve homogeneity. The average wt% Y and one standard deviation from all analysis points was found to be 0.214±0.170, 0.215±0.474, and 0.154±0.089 for the as-received Ar, Ar/O, and He atomized powders, respectively. After MA, the EPMA analysis shows much improved average and standard deviation values for Y of 0.206±0.027, 0.250±0.048, 0.196±0.035 for Ar, Ar/O, and He, respectively.

TEM and EDS showed the presence of large elongated and spherical Y rich features between 20 nm and 100 nm in all of the atomized powder variants. An example image of the He atomized powder is shown in Figure 1. Variations in size, morphology, and composition of the Y-rich precipitates were observed. Likely candidate phases include intermetallic Y_2Fe_{17} and complex yttrium oxides, as suggested by the EDS spectra shown in Figure 1.

SANS measurements showed almost no scattering in the high q-range associated with NF in the as-atomized powders compared to the control specimen. Only a small amount of additional scattering was present in the milled powders. In contrast, similar NF scattering was observed in all the powder variants after annealing, as shown in Figure 2a. Here the scattering cross section 45° to the magnetic axis is shown for the 3 powder variants in the milled and annealed condition, along with the Y-free milled and annealed control. Note the 45° curve represents the sum of the nuclear plus half the magnetic scattering. The large bulge in the scattering below $q \approx 2.5\ nm^{-1}$ is due to scattering of nm-scale features. Fits to the Ar atomized data showed a precipitate radius, volume fraction and number density of 1.5 nm, 1.47%, and 9.9 $X10^{23}/m^3$, which are comparable to other NFA materials such as MA957 [3]. This is shown in Figure 2b comparing the Ar atomized, milled and annealed powder with scattering curves for commercial vendor MA957 and previous data for powders that had been milled with Y_2O_3.

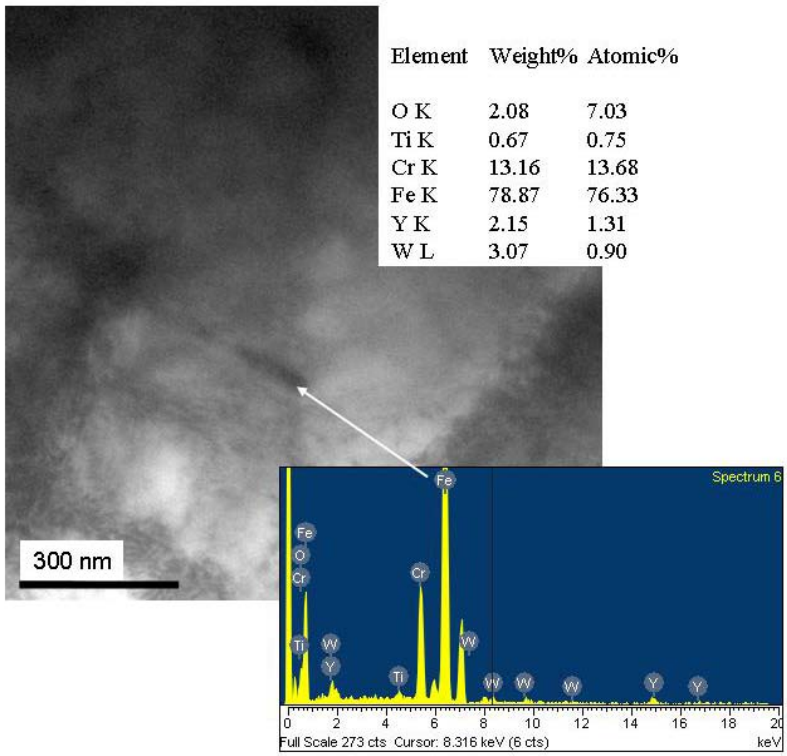

Fig. 1 Elongated Y-enriched feature in an as-received He atomized powder.

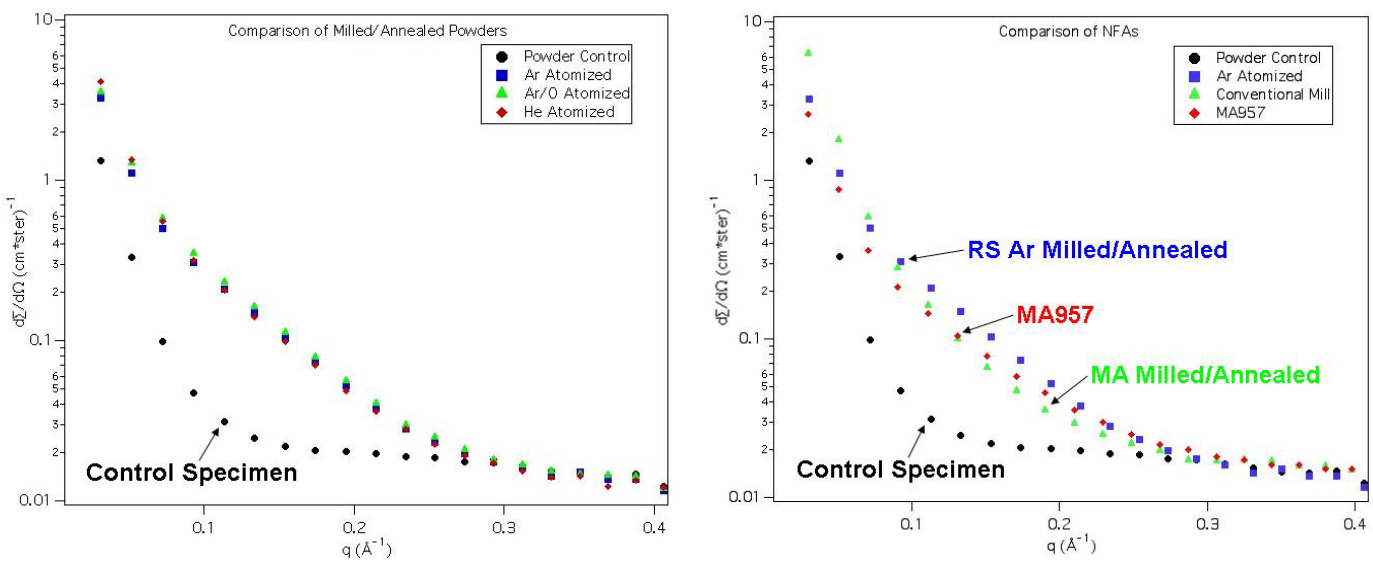

Fig. 2 a) Comparison of absolute scattering between Ar, Ar/O, and He atomized milled/annealed powders; b) Comparison of Ar atomized milled/annealed powder with MA957 and conventional MA milled/annealed powder.

SEM showed a bimodal grain size distribution in all three variants of the milled and annealed powders. Previous research suggested that the larger grains have a very low density of NF [including Hoelzer]. However, shown in Figure 3, APT found NF in both small and large grains in the Ar atomized milled and annealed powders. Eiselt et

al. recently reported a similar observation [8, 9]. The solute contents of the NF were similar, with average Y/Ti/O ratios of 30/30/40 for the small grains and 26/33/41 for the large grains. The number density of the precipitates was found to be 3.3 $X10^{23}/m^3$ and 7.5 $X10^{23}/m^3$ for small and large grains, respectively. These results compare well with TEM and SANS measurements of other NFA.

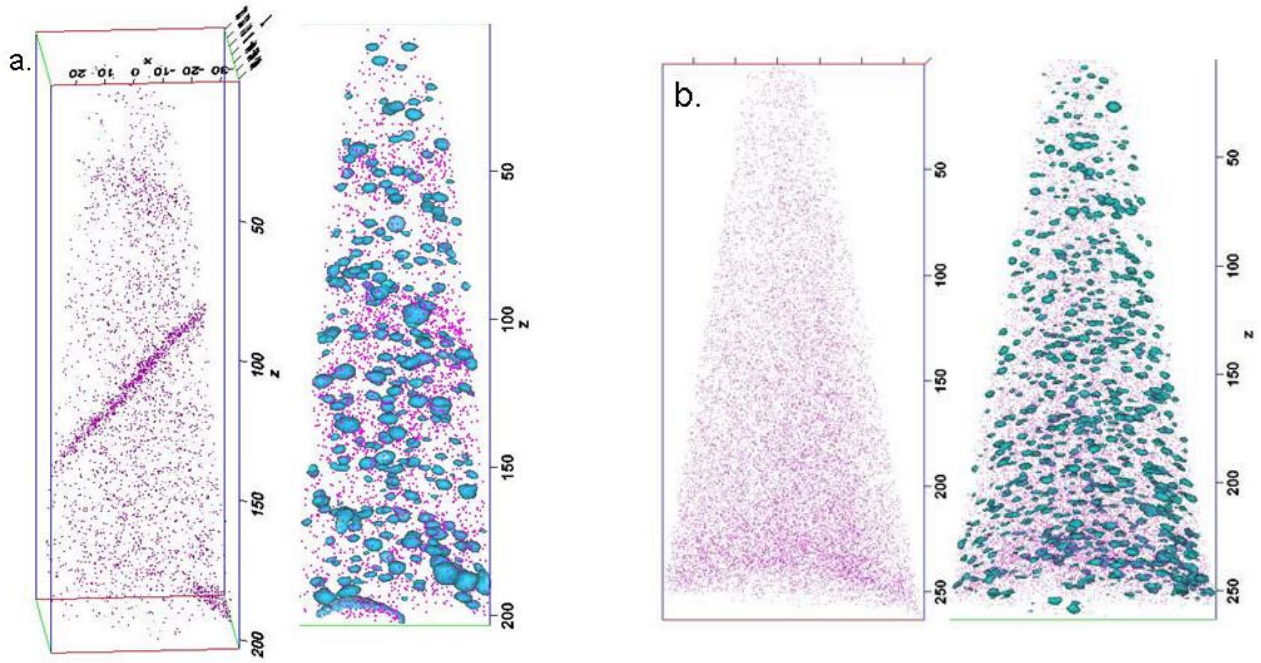

Fig. 3 (a) Phosphorus segregation and NFs in small grains in the Ar atomized milled/annealed sample and (b) NFs unexpectedly present in large grain.

Summary

The Y distribution in three variants of Fe14Cr3W0.3Ti0.2Y rapidly solidified powders was characterized at UCSB by TEM, EPMA, APT and SANS in the as atomized, MA, and MA/annealed conditions. Rapid solidification in all three atmospheres of Ar, Ar/O, and He produce large Y-enriched features and non-uniform Y distributions on a µm scale. While there are some apparent differences in their size, morphology and composition, TEM and EDS show Y rich particles between 0.02 and 0.1 µm in all three of the powder variants. However, SPEX ball milling for 10 h produces a uniform distribution of Y. The Y clusters along with O and Ti during annealing at 1100°C produce a high density of NF. There is a bimodal grain size distribution in all of the milled and annealed powders. Notably, Y-Ti-O precipitates are present in both the large and small grains. The size, number density, volume fraction and composition of the NF compare favorably to those found in other NFA, such as MA957.

Future Research

A large heat of Ar atomized 0.2Y powders will be prepared by CR. After systematic characterization and small batch processing studies are completed, the powders will be milled and consolidated by a best practice processing route.

References

1. G.R. Odette, M.J. Alinger, and B.D. Wirth, Annual Review of Materials Research, Vol. 38, (2008).
2. P. Miao, G.R. Odette, T. Yamamoto, M.J. Alinger, D.T. Hoelzer, and D. Gragg, J. of Nucl. Mater., 367–370 (2007) 208–212.
3. M. J. Alinger, On the Formation and Stability of Nanometer Scale Precipitates in Ferritic Alloys during Processing and High Temperature Service, Thesis (PhD), University of California Santa Barbara (2004).
4. C.J. Glinka, J.G. Barker, B. Hammouda, S. Krueger, J.J. Moyer, and W.J. Orts, J. Appl. Cryst., 31, (1998), 430-445.

5. M.J. Alinger, G.R. Odette, and D.T. Hoelzer, Acta Mater, 57 (2009), 392-406.
6. A.M. Harris, G.B. Schaffer, and N.W. Page, J. Mater. Science Letters, 12, (1993), 160-161.
7. M.K. Miller, Atom Probe Tomography: analysis at the atomic level, Kluwer Academic/Plenum, New York, (2000).
8. C.C. Eiselt, M. Klimenkov, R. Lindau, A. Möslang, H.R.Z. Sandim, A.F. Padilha, and D. Raabe, J. Nucl. Mater., 385 (2009) 231-235.
9. C.C. Eiselt, M. Klimenkov, R. Lindau, and A. Möslang, J. Nucl. Mater., 386-388 (2009) 525-528.